Nuclear response for the Skyrme effective interaction with zero-range tensor terms. III. Neutron matter and neutrino propagation

A. Pastore,[1,*] M. Martini,[2,†] V. Buridon,[1,‡] D. Davesne,[1,§] K. Bennaceur,[1,‖] and J. Meyer[1,¶]

[1]*Université de Lyon, F-69003 Lyon, France, Université Lyon 1, 43 Bd. du 11 Novembre 1918, F-69622 Villeurbanne cedex, France and CNRS-IN2P3, UMR 5822, Institut de Physique Nucléaire de Lyon, F-69622 Villeurbanne cedex, France*

[2]*Institut d'Astronomie et d'Astrophysique, CP-226, Université Libre de Bruxelles, 1050 Brussels, Belgium*

(Received 17 July 2012; published 8 October 2012)

The formalism of the linear response for the Skyrme energy density functional including tensor terms derived in Refs. [1,2] for nuclear matter is applied here to the case of pure neutron matter. As in Ref. [2] we present analytical results for the response function in all channels, the Landau parameters, and the odd-power sum rules. Special emphasis is given to the inverse energy weighted sum rule because it can be used to detect nonphysical instabilities. Typical examples are discussed and numerical results shown. Moreover, as a direct application, neutrino propagation in neutron matter is investigated through its neutrino mean-free path at zero temperature. This quantity turns out to be very sensitive to the tensor terms of the Skyrme energy density functional.

DOI: 10.1103/PhysRevC.86.044308 PACS number(s): 21.30.Fe, 21.60.Jz, 21.65.Cd, 26.60.Kp

I. INTRODUCTION

In a recent series of articles [1,2], hereafter denoted respectively article I and II, the contribution of the zero-range tensor terms in the Skyrme effective interaction has been analyzed in the context of the linear response theory. The first result from these articles is that the tensor terms have very sizable effects on the response functions. Another important result is that the inverse energy weighted sum rule can be used as a tool of diagnosis for instabilities. These two articles were devoted to symmetric nuclear matter (SNM) only. Since the construction of an energy density functional (EDF) reliable for both symmetric matter and neutron matter is of fundamental importance [3,4], we present here the response functions and some associated sum rules for pure neutron matter (PNM) with the same approach. The interest of the present study is related to spin susceptibilities and ferromagnetic finite size instabilities in neutron matter [5–21]. Moreover, we use these results to study the impact of the tensor terms on the determination of the neutrino mean-free path in PNM. This is a quantity of intrinsic importance since the cooling of a neutron star core in its first moments is governed by neutrino emission and therefore by their mean-free path through dense matter. Some previous studies using nonrelativistic approaches [22–27] have revealed some very interesting features of the mean-free-path properties but they usually neglected the possible tensor contribution. Since the neutrino mean-free path is directly related to the response functions which are themselves affected by the tensor, it is worthwhile to determine precisely the induced modifications [28,29].

The article is organized as follows: in the first part devoted to the linear response theory approach, we present explicit expressions for the spin response functions, the Landau parameters, and the sum rules M_1, M_3, M_{-1}. Since the technical approach follows closely that of the previous articles, this part mainly contains figures and discussion; the formulas are written in the appendices. The second part deals with the problem of the neutrino mean-free path. We first give an explicit expression of this quantity in the presence of tensor interactions, then we show the influence of the parametrizations of the Skyrme functional.

II. LINEAR RESPONSE APPROACH TO NEUTRON MATTER

A. Response function

Following article II, the starting point for the determination of the response functions is the Skyrme energy functional. Since in neutron matter the isospin is no longer a relevant quantum number and isovector and isoscalar densities are equal, it is convenient to define new coupling constants $C^x = C_0^x + C_1^x$, where $x = \rho, \tau, \Delta\rho, \ldots$ in such a way that the energy density functional can be written as

$$E = \int \mathcal{E} \mathrm{d}^3 r, \tag{1}$$

with

$$\begin{aligned}\mathcal{E} = {} & C^{\rho}[\rho]\,\rho^2 + C^{\Delta\rho}\rho\Delta\rho + C^{\tau}(\rho\tau - \mathbf{j}^2) \\ & + C^{s}[\rho]\,\mathbf{s}^2 + C^{\nabla \mathbf{s}}(\boldsymbol{\nabla}\cdot\mathbf{s})^2 + C^{\Delta s}\mathbf{s}\cdot\Delta\mathbf{s} \\ & + C^{T}\left(\mathbf{s}\cdot\mathbf{T} - \sum_{\mu\nu=x}^{z} J_{\mu\nu}J_{\mu\nu}\right) \\ & + C^{F}\left[s\cdot\mathbf{F} - \frac{1}{2}\left(\sum_{\mu=x}^{z} J_{\mu\mu}\right)^2 - \frac{1}{2}\sum_{\mu\nu=x}^{z} J_{\mu\nu}J_{\nu\mu}\right] \\ & + C^{\nabla J}\left[\rho\boldsymbol{\nabla}\cdot\mathbf{J} + \mathbf{s}\cdot(\boldsymbol{\nabla}\times\mathbf{j})\right].\end{aligned} \tag{2}$$

The expressions of the coupling constants as functions of the parameters of the Skyrme interaction can be found in article I. From this expression, it is straightforward to obtain

*pastore@ipnl.in2p3.fr
†mmartini@ulb.ac.be
‡v.buridon@ipnl.in2p3.fr
§davesne@ipnl.in2p3.fr
‖bennaceur@ipnl.in2p3.fr
¶jmeyer@ipnl.in2p3.fr

the residual interaction (see table in Appendix A) by taking the second derivative of the EDF with respect to the density.

The random phase approximation (RPA) response function in each channel $(\alpha) = (S, M) \equiv$ (spin, projection of the spin) (see Appendix B) is then obtained by solving the Bethe-Salpeter equations for the correlated Green functions $G^{(\alpha)}_{\rm RPA}$. Finally, from this residual interaction, we can easily obtain the Landau parameters (see Appendix C). The quantities of interest are not directly the RPA propagators themselves, but merely the response functions $S^{(\alpha)}(\mathbf{q}, \omega)$, also called the dynamical structure functions by some authors, which are defined at zero temperature by

$$S^{(\alpha)}(\mathbf{q}, \omega) = -\frac{1}{\pi}\mathrm{Im}\chi^{(\alpha)}(\mathbf{q}, \omega). \tag{3}$$

From now on we choose the direction of $\mathbf{q}$ along the z axis, as done in articles I and II. We show this function in Fig. 1 for two different values of the transferred momentum ($q = 0.05$ fm^{-1} and $q = 0.5$ fm^{-1}) and two different densities ($\rho = 0.08$ fm^{-3} and $\rho = 0.16$ fm^{-3}) as a function of the energy ω. As in articles I and II we use a system of natural units so that $\hbar = c = 1$. We consider one interaction without tensor, (i.e., SLy5) and one with tensor, T16 (see the article of Lesinski *et al.* [30] for the definition of the TIJ parametrizations). Among the several TIJ possibilities the choice of T16 is motivated by the study of the neutrino mean-free path (see below). In order to illustrate the effect of the interaction and of the RPA correlations we plot in each panel the corresponding Fermi gas (FG) and Hartree-Fock results (i.e., uncorrelated response functions). A first effect of the interaction clearly appears at the Hartree-Fock level where the mean field is responsible for the dressing of the bare neutron mass giving a density-dependent effective one. The difference between the Fermi gas and the Hartree-Fock structure functions increases with the density. With the RPA correlations, the difference between the $S = 0$ and $S = 1$ channel of the p-h interaction are reflected in the corresponding response functions. Let us focus on the $S = 1$ channel, particularly important for the neutrino mean-free path. The $(S = 1, M = 0)$ and $(S = 1, M = 1)$ structure functions practically coincide, as it is expected for the SLy5 force, while they clearly differ in the presence of tensor interaction. The small difference between the $(S = 1, M = 0)$ and $(S = 1, M = 1)$ structure functions in the case of SLy5 is only due to the spin-orbit contribution and according to Eqs. (B5) and (B8) given in Appendix B, their contribution is proportional to the factor q^4 and thus is less important for low transfer momenta. Concerning $S = 1$ for low q (as illustrated in the figure for $q = 0.05$ fm^{-1}), a spin zero-sound mode appears. It stands out above the p-h continuum. The existence of this spin collective mode, called magnon, makes the excitation of the system more difficult; hence, correspondingly the p-h continuum response is depleted. This antiferromagnetic behavior disappears when q increases. For high q another kind of divergence may appear. As illustrated in Fig. 2, the enhancement of the response function may become dramatic and show a pole at $\omega = 0$. In this case the homogeneous Hartree-Fock ground state becomes unstable. For lower values of q the same kind of instability appears at higher density, called the critical density ρ_c, as illustrated in the next section.

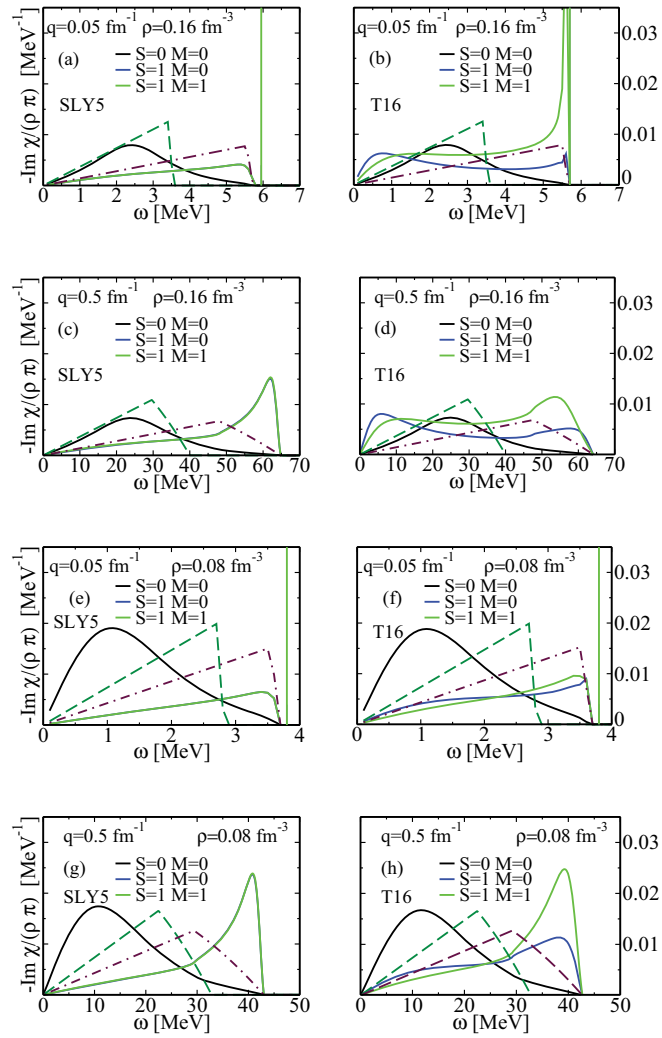

FIG. 1. (Color online) For the three PNM channels, we show the response functions $S^{(\alpha)}(q, \omega)$ for the interaction SLy5 and T16. The vertical lines represent the position of the eventual zero-sound mode. For each force we plot as a reference the Fermi gas response function (dashed line) and the uncorrelated response function (dash-dotted line).

B. Sum rules and moments of strength function

Following the notations of article II, we can calculate the most relevant odd-power sum rules for PNM, in particular the M_1 energy-weighted sum rule (EWSR), the M_3 cubic energy-weighted sum rule (CEWSR) and the M_{-1} inverse energy-weighted sum rule (IEWSR) defined as

$$M^{(\alpha)}_k(q) = \int_0^\infty \mathrm{d}\omega\omega^k S^{(\alpha)}(q, \omega). \tag{4}$$

As stated previously, all the expressions given below are derived for the general Skyrme EDF given by Eq. (2) in which all the coupling constants could be considered as independent

from the others. We refer to article II for a detailed discussion on their derivation.

The EWSR in each channel reads

$$M_1^{(0,0)} = \frac{q^2}{2m^*}\left(1 - W_2^{(0)} m^* \rho\right), \tag{5}$$

$$M_1^{(1,0)} = \frac{q^2}{2m^*}\left[1 - \left(W_2^{(1)} + 2C^F\right) m^* \rho\right], \tag{6}$$

$$M_1^{(1,\pm1)} = \frac{q^2}{2m^*}\left(1 - W_2^{(1)} m^* \rho\right). \tag{7}$$

Taking into account the $W_2^{(0)}$ value as well as the neutron effective mass m^*, defined as

$$\frac{m}{m^*} = 1 + 2m\left(C_0^\tau + C_1^\tau\right)\rho, \tag{8}$$

the $M_1^{(0,0)}$ EWSR reduces to the free value $q^2/(2m)$, as it should. As in article II for the case of a Skyrme force, these M_1 moments can be obtained from the double commutator method [39,40].

For the CEWSR we have

$$M_3^{(0,0)} = q^4 \frac{k_F^2}{2m^{*3}}\left[1 - m^*\rho W_2^{(0)}\right]^2 \left\{\frac{3}{5} + k^2 + k^2 m^* \rho W_2^{(0)} + \frac{m^*\rho}{2k_F^2}\left[W_1^{(0)} + 2k_F^2 W_2^{(0)}\right]\right\}, \tag{9}$$

$$M_3^{(1,0)} = q^4\rho^2[C^F]^2\frac{k_F^2}{5tm^*}\left\{2m^*\rho\left[W_2^{(1)} + 2C^F\right] - 1\right\} + q^4\frac{k_F^2}{2m^{*3}}\left\{m^*\rho\left[W_2^{(1)} + 2C^F\right] - 1\right\}^2$$
$$\times\left\{\frac{3}{5} + k^2 + \frac{6}{5}m^*\rho C^F + k^2 m^*\rho W_2^{(1)} + \frac{m^*\rho}{2k_F^2}\left[W_1^{(1)} + 4q^2 C^{\nabla s} + 2k_F^2 W_2^{(1)}\right]\right\}, \tag{10}$$

$$M_3^{(1,\pm1)} = q^4\rho^2[C^F]^2\frac{k_F^2}{10m^*}\left\{2m^*\rho W_2^{(1)} - 1\right\} + q^4\frac{k_F^2}{2m^{*3}}\left[m^*\rho W_2^{(1)} - 1\right]^2$$
$$\times\left\{\frac{3}{5} + k^2 + \frac{2}{5}m^*\rho C^F + k^2 m^*\rho W_2^{(1)} + \frac{1}{2}\frac{m^*\rho}{k_F^2}\left[W_1^{(1)} + 2k_F^2 W_2^{(1)}\right]\right\}. \tag{11}$$

And finally for the IEWSR we have

$$M_{-1}^{(0,0)} = f(k)\frac{3m^*}{2k_F^2}\left\{-24k^2[m^*\rho C^{\nabla J}]^2\frac{f(k)[1 - 3(k^2-1)f(k)]}{4 - m^*\rho[1 - 3(k^2-1)f(k)]\left[W_2^{(1)} - C^F\right]} - \frac{3}{16}\left[m^*\rho f(k)\left(k^2-1\right)W_2^{(0)}\right]^2\right.$$
$$\left. + f(k)\left[\frac{k_F m^*}{2\pi^2}W_1^{(0)} + \frac{3}{2}m^*\rho(1-k^2)W_2^{(0)} - \frac{1}{8}(3+13k^2)\left[m^*\rho W_2^{(0)}\right]^2\right] + \left[1 + \frac{3}{4}m^*\rho W_2^{(0)}\right]^2\right\}^{-1}, \tag{12}$$

$$M_{-1}^{(1,0)} = f(k)\frac{3m^*}{2k_F^2}\left\{\left[1 + \frac{1}{4}m^*\rho\left(3W_2^{(1)} + 4C^F\right)\right]^2 - \frac{3}{16}[m^*\rho f(k)(k^2-1)]^2\left[W_2^{(1)}\right]^2\right.$$
$$+ f(k)\left[\frac{k_F m^*}{2\pi^2}\left[W_1^{(1)} + 4q^2 C^{\nabla s}\right] - \frac{3}{2}m^*\rho\left(4k^2 C^F + (k^2-1)W_2^{(1)}\right)\right.$$
$$\left.\left. - \frac{1}{8}m^{*2}\rho^2\left(24(1+k^2)[C^F]^2 + 12(1+3k^2)C^F W_2^{(1)} + (3+13k^2)\left[W_2^{(1)}\right]^2\right)\right]\right\}^{-1}, \tag{13}$$

$$M_{-1}^{(1,\pm1)} = f(k)\frac{3m^*}{2k_F^2}\left\{-12[m^*\rho C^{\nabla J}]^2\frac{k^2 f(k)[1 + 3f(k)(1-k^2)]}{4 - m^*\rho[1 + 3f(k)(1-k^2)]W_2^{(0)}}\right.$$
$$+ \left[1 + \frac{1}{4}m^*\rho\left(3W_2^{(1)} + C^F\right)\right]^2 - \frac{3}{16}[m^*\rho f(k)(1-k^2)]^2\left(5[C^F]^2 + 2C^F W_2^{(1)} + \left[W_2^{(1)}\right]^2\right)$$
$$+ f(k)\left[\frac{k_F m^*}{2\pi^2}W_1^{(1)} + \frac{3}{2}m^*\rho(1-k^2)\left[W_2^{(1)} + C^F\right]\right.$$
$$\left.\left. + \frac{1}{8}m^{*2}\rho^2\left([C^F]^2(k^2-9) - 8k^2 C^F W_2^{(1)} - (3+13k^2)\left[W_2^{(1)}\right]^2\right)\right]\right\}^{-1}, \tag{14}$$

where the $W_{i=1,2}^{(S)}$ coefficients are given in Appendix B.

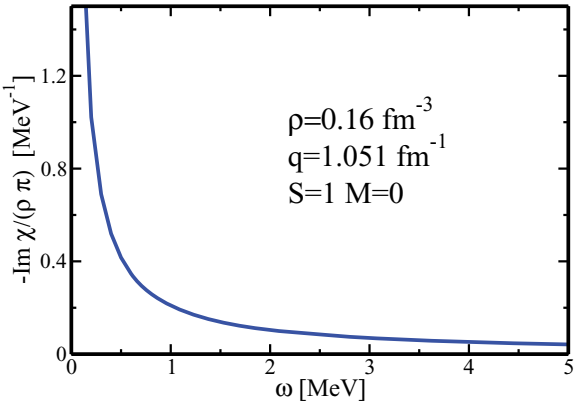

FIG. 2. (Color online) Response functions $S^{(\alpha)}(q,\omega)$ calculated for Skyrme tensor parametrization T16 [30], for channel $S=1$, $M=0$ only. The transfer momentum is $q=1.051$ fm^{-1} and the density of the system is $\rho=0.16$ fm^{-3}.

As in article II we define the function $f(k)$ as

$$f(k)=\frac{1}{2}\left[1+\frac{1}{2k}(1-k^2)\ln\left(\frac{k+1}{k-1}\right)\right], \qquad (15)$$

while ρ and k are now defined for PNM with Fermi momentum k_F, hence

$$\rho=\frac{1}{3\pi^2}k_F^3, \quad k=\frac{q}{2k_F}.$$

As already illustrated in the previous section, the main effect of the tensor terms is in the $S=1$ channel where one can even observe a divergence at zero energy, but finite transferred momentum. As explained in detail in article II, the IEWSR M_{-1} can be used to detect these poles. As an example, in Fig. 3, we plott the IEWSR for T16 obtained from the analytic expansion of the response function [see Eqs. (12)–(14)] and from the direct numeric integration. We observe on this figure

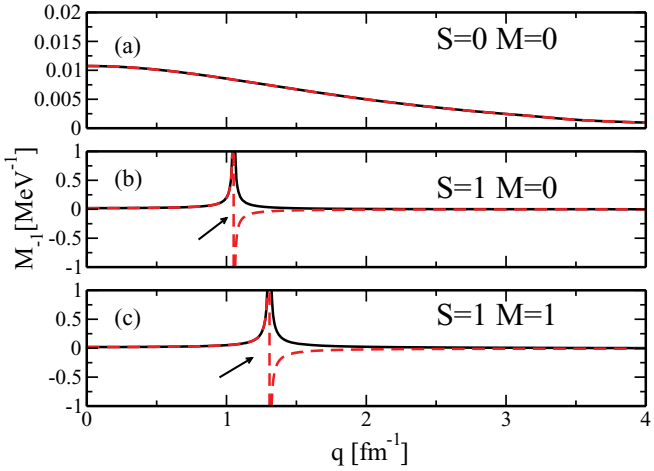

FIG. 3. (Color online) IEWSR (in MeV^{-1}) as a function of transferred momentum q (in fm^{-1}) for T16 tensor parametrization. Full black line shows the result of the integral Eq. (4) while the dashed red line shows the result of the analytical expression (12)–(14). The results are obtained at $\rho=0.16$ fm^{-3}. The arrow indicates the position of the instability.

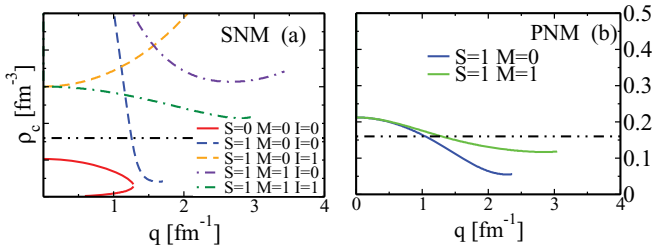

FIG. 4. (Color online) Critical densities (in fm^{-3}) as functions of the transferred momentum q (in fm^{-1}) for the T16 tensor parametrization and for SNM [panel (a)] and for PNM [panel (b)]. The horizontal dash-dotted line is placed at $\rho=0.16$ fm^{-3} just to guide the eye.

that, in the channels $S=1$, $M=0$ and $S=1$, $M=1$, the IEWSR is violated. This indicates the presence of a pole in the response function as shown for example for $S^{(1,0)}(q,\omega)$ in Fig. 2 for $\rho=0.16$ fm^{-3} and transferred momentum $q=1.051$ fm^{-1}.

This connection between the pole (when it does exist) observed in the response function and the pole observed in the M_{-1} sum rule has been discussed in article II and we refer to it for a more detailed discussion on this point. It is thus possible to determine in a systematic way the critical density at which a pole occurs for a given momentum q from Eqs. (12)–(14). In Fig. 4 we display such critical densities ρ_c with respect to the transferred momentum for the T16 interaction. In the left panel we first show the position of the poles of the response function for SNM for each (S,M,I) channel. In the right panel we then show the position of the poles for PNM for each (S,M) channel.

Even if we exclude the case of spinodal instability which is not present in PNM, one can see that the presence and the location of the poles depends strongly on the system under analysis: for a given interaction, the critical densities are very different for PNM and SNM. Similarly, we show in Fig. 5 the

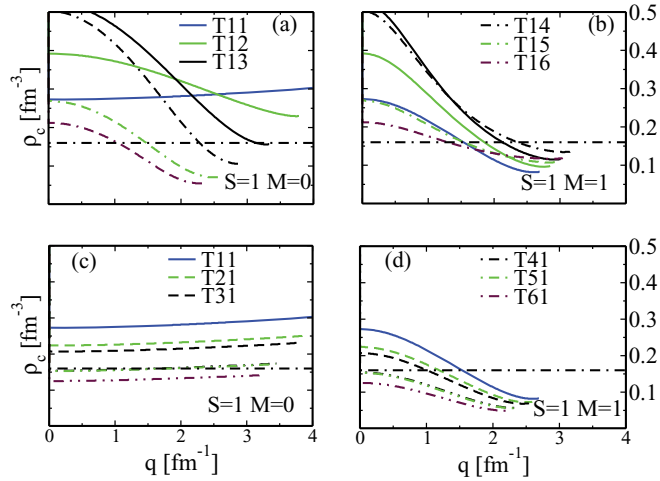

FIG. 5. (Color online) For the two $S=1$ channels in PNM, critical densities (in fm^{-3}) are plotted as functions of the transferred momentum q (in fm^{-1}) for the TIJ family of Skyrme forces. The horizontal dash-dotted line is placed at $\rho=0.16$ fm^{-3} just to guide the eye.

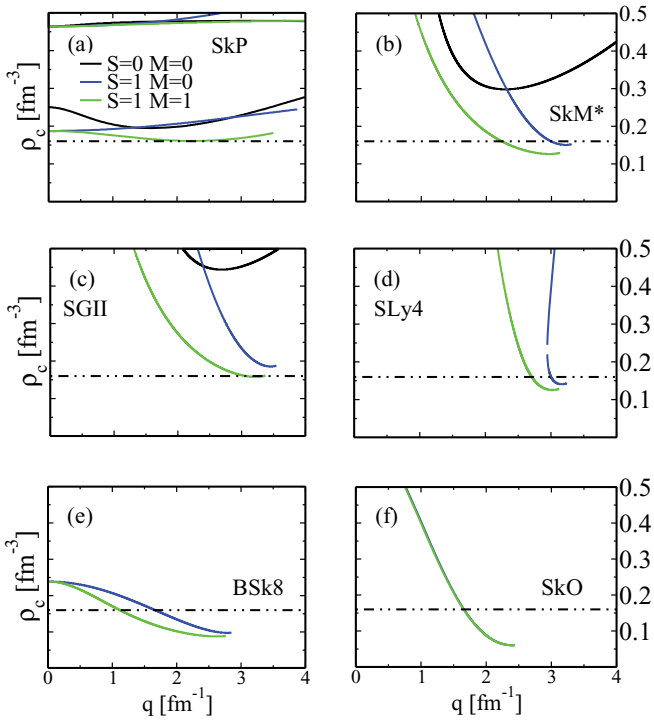

FIG. 6. (Color online) For the three PNM channels, critical densities (in fm^{-3}) are plotted as functions of transferred momentum q (in fm^{-1}) for some usual Skyrme EDF: SkP [31], SkM* [32], SGII [33], SLy4 [34–36], BSk8 [37], and SkO [38]. The horizontal dash-dotted line is placed at $\rho = 0.16\ \mathrm{fm}^{-3}$ just to guide the eye.

critical densities for the tensor parametrizations that we use in the following section to study the neutrino mean-free path.

Following article II, we show for completeness in Fig. 6 the critical densities for the Skyrme EDF previously analyzed in article II for SNM, but in this case for PNM. We observe that SkP behaves very differently from the other Skyrme forces presented in this article. It presents a first instability in the $S = 0$ channel at $\rho \approx 0.16\ \mathrm{fm}^{-3}$ and a second one at higher density at $\rho \approx 0.45\ \mathrm{fm}^{-3}$ due to the presence of a pole in the effective mass defined in Eq. (8).

III. NEUTRINO MEAN-FREE PATH

The aim of this section is to investigate the effect of the choice of the parameters of the tensor terms on the neutrino mean-free path in neutron matter. In this article we restrict ourselves to the academic case of neutron matter at zero temperature (the generalization at finite temperature T is in progress). This, of course, implies some restriction on the application of our approach to neutron stars studies. At first stages of the cooling process of the neutron stars, modelized as asymmetric nuclear matter, the high temperatures involved allow charged current reactions; then, when the temperature decreases, neutral currents dominate. Since we consider the case $T = 0$ and the pure neutron matter, we will take into account only neutral currents for the determination of the neutrino mean-free path. This quantity is defined as

$$\lambda = (\sigma\rho)^{-1}, \tag{16}$$

where σ is the total cross section for the neutral current reaction $\nu + n \longrightarrow \nu' + n'$. In the absence of tensor (and spin-orbit) interaction this total cross section is obtained by integrating the double differential cross-section per neutron

$$\frac{d^2\sigma(E_\nu)}{d\Omega_{k'}d\omega} = \frac{G_F^2 E_\nu'^2}{16\pi^2}\left[(1+\cos\theta)\,R^V(q,\omega) + g_A^2\,(3-\cos\theta)\,R^A(q,\omega)\right], \tag{17}$$

where G_F is the weak coupling constant, $g_A = 1.255$ [41] is the axial charge of the nucleon, E_ν and E'_ν are the incoming and outgoing neutrino energies, respectively, θ is the scattering angle between the incoming and outgoing neutrino momenta, and $\omega = E_\nu - E'_\nu$ and $\mathbf{q} = \mathbf{k} - \mathbf{k}'$ are the energy and momentum transfer in the reaction. The response functions $R^V(q,\omega)$ and $R^A(q,\omega)$ describe the response of the system to density fluctuations ($S = 0$) and spin fluctuations ($S = 1$) related to the coupling of neutrino to vector and axial currents of the neutron. These response functions are defined as

$$\begin{aligned} R^V(q,\omega) &= -\frac{1}{\pi\rho}\mathrm{Im}\chi^{(S=0)}(q,\omega), \\ R^A(q,\omega) &= -\frac{1}{\pi\rho}\mathrm{Im}\chi^{(S=1)}(q,\omega). \end{aligned} \tag{18}$$

When tensor forces are considered the spin response is split into two components; namely, the spin longitudinal response

$$R_L^A(q,\omega) = -\frac{1}{\pi\rho}\mathrm{Im}\chi^{(S=1,M=0)}(q,\omega), \tag{19}$$

and the spin transverse response

$$R_T^A(q,\omega) = -\frac{1}{\pi\rho}\mathrm{Im}\chi^{(S=1,M=\pm1)}(q,\omega). \tag{20}$$

These responses can be considerably different one from the other and compared to the case without tensor interaction. This has important consequences on the neutrino cross sections and the neutrino mean-free path. In the presence of tensor interaction the double differential cross-section per neutron for neutral current reaction is given by

$$\frac{d^2\sigma(E_\nu)}{d\Omega_{k'}d\omega} = \frac{G_F^2 E_\nu'^2}{16\pi^2}\left\{(1+\cos\theta)R^V + g_A^2\left[\frac{2(E'_\nu\cos\theta - E_\nu)(E'_\nu - E_\nu\cos\theta)}{q^2} + 1 - \cos\theta\right]R_L^A + g_A^2 2\left[\frac{E_\nu E'_\nu}{q^2}\sin^2\theta + 1 - \cos\theta\right]R_T^A\right\}. \tag{21}$$

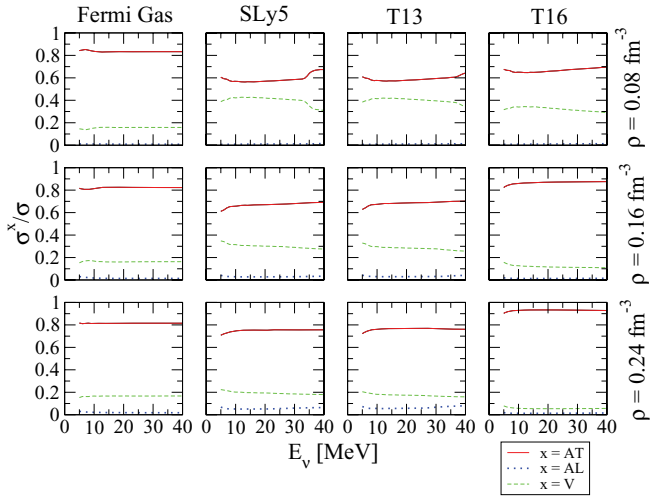

FIG. 7. (Color online) Relative axial spin transverse (AT), relative axial spin longitudinal (AL), and relative vector (V) contributions to the cross section per neutron for the reaction $\nu + n \longrightarrow \nu' + n'$ in the neutron matter. Three different densities as well three different interactions are considered. The Fermi gas result is also shown.

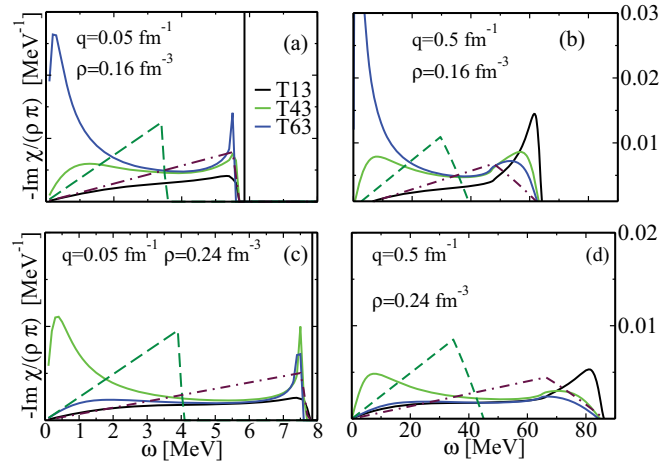

FIG. 8. (Color online) The response functions for the channel $S = 1$, $M = 1$ for three different forces (T13, T43, and T63) is shown with solid lines. On the same figure we represent the Fermi gas (dashed line) and the uncorrelated response functions (dash dotted; i.e., when the residual interaction is put to zero), for the interaction T13. The uncorrelated response functions are not equivalents among T13, T43, and T63 due to the small differences in the effective mass.

This expression reduces to Eq. (17) when $R_L^A = R_T^A = R^A$ as one can easily observe remembering that for neutral current

$$q^2 = (\mathbf{k} - \mathbf{k}')^2 = k^2 + k'^2 - 2\mathbf{k}\cdot\mathbf{k}' = E_\nu^2 + E_\nu'^2 - 2E_\nu E_\nu' \cos\theta. \quad (22)$$

In Eq. (21), as well as in Eq. (17), we neglect corrections of order E_ν/m from weak magnetism and other effects [42] like the finite size of the nucleon or nucleon excitations [43]. A generalization of Eq. (21) taking into account all these effects can be found, for example, in Ref. [41]. As already stressed in Ref. [41] (and illustrated in Ref. [44] for charged current reaction) the cross section is dominated by the spin transverse response R_T^A. In Fig. 7 we present the relative axial spin transverse, axial spin longitudinal, and vector contributions to the neutral current cross section. We consider four different cases. The first is the Fermi gas. In this case $R_L^A = R_T^A = R^A$ so the difference between the three contributions is only due to the kinematical factors and the coupling constants multiplying the response functions. Second we consider the case when the response functions are calculated with the SLy5 force. In this case the coupling constants $C^F = C^{\nabla s} = 0$, purely related with the tensor part of the interaction, do not contribute. A possible difference between R_L^A and R_T^A is due to the spin orbit contribution and according to Eqs. (B5) and (B8) given in Appendix B, the q^4 factor reduces these differences at low momentum transfer. Finally, we consider the T13 and T16 parametrizations of tensor contributions. The results for three different densities, $\rho = 0.08$, 0.16, and 0.24 fm^{-3} are also shown in Fig. 7. As clearly appears, all the cross sections are dominated by the spin transverse response but this contribution may vary between ∼60% and ∼90% depending on the interactions and densities considered. It reflects possible quenching, enhancement or divergence of the nuclear response functions. This behavior was already illustrated in Sec. II A in connection with Fig. 1. To complete our discussion we plot in Fig. 8 the spin transverse response for $q = 0.05$ fm^{-1} and $q = 0.5$ fm^{-1}, for $\rho = 0.16$ fm^{-3} and $\rho = 0.24$ fm^{-3} and for the tensor forces T13, T43, and T63. A collective spin zero sound characterizes the $S = 1$, $M = \pm 1$ response for T13 at $q = 0.05$ fm^{-1} for $\rho = 0.16$ fm^{-3} and $\rho = 0.24$ fm^{-3}. A similar behavior, with the corresponding quenching of the p-h continuum characterizes the $S = 1$, $M = \pm 1$ responses for SLy5 and T16 as shown in Fig. 1 for $\rho = 0.08$ fm^{-3} and $\rho = 0.16$ fm^{-3}. The T63 force on the other hand is characterized by an enhancement of the response at low ω for $\rho = 0.16$ fm^{-3}. At $q = 0.5$ fm^{-1} this enhancement seems to be critical. At $\rho = 0.24$ fm^{-3} the enhancement of the T16 response no longer holds. In this case this response is suppressed with respect to the corresponding Hartree-Fock response. An enhancement with respect to the HF and FG case for small ω characterizes for this density the T43 force.

These different behaviors obviously affect the neutrino mean-free path. We have calculated it for T11-T16 and T13-T63 chains of parametrizations of Skyrme tensor interactions for a neutrino energy 5 MeV $< E_\nu <$ 40 MeV and for three values of densities (i.e., $\rho = 0.08$, 0.16, and 0.24 fm^{-3}). Note that when a spin zero-sound collective mode appears one must in principle include it in the calculation of the neutrino mean-free path. For this mode the response function reduces to a delta distribution. Nevertheless, as already observed in Ref. [22], the collective mode itself gives little scattering, its contribution is negligible when calculated in the Landau approximation. It was also observed in Ref. [24] that for all the Skyrme forces considered, this magnon rapidly disappears with temperature because of strong Landau damping. Hence we do not explicitly compute the spin zero-sound contribution. Its effect is, on the other hand, present as a suppression of the corresponding p-h continuum and has a consequence on the cross section.

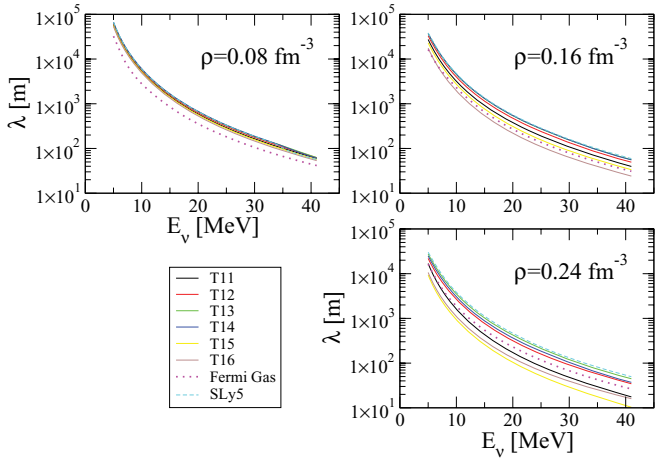

FIG. 9. (Color online) Neutrino mean-free path for scattering reaction $\nu + n \longrightarrow \nu' + n'$ in neutron matter. The dotted lines correspond to the noninteracting Fermi gas case. The dashed lines are the interacting case with the SLy5 force. The continuous lines correspond to several parametrizations of the tensor contribution following the T11–T16 chain. The system densities considered in the three panels are $\rho = 0.08$, 0.16, and 0.24 fm^{-3}.

The results for the neutrino mean-free path are reported in Fig. 9 for the T11–T16 chain and in Fig. 10 for the T13–T63 chain. In each figure we include the Fermi gas result and the calculation with the SLy5 force which does not have tensor terms. From Figs. 9 and 10 clearly emerges the crucial dependence of the neutrino mean-free path on the parametrizations of the Skyrme tensor terms. For $\rho = 0.08$ fm^{-3} the different parametrizations give quite similar results and higher with respect to the noninteracting case. Already at $\rho = 0.16$ fm^{-3} the spread becomes important. For some cases λ is higher than the Fermi gas case; for others it is lower. In many cases it is lower than the corresponding SLy5 result. Also the behavior of λ with the density is not so trivial, as already appears in the three panels of Figs. 9 and 10. This is clearly shown in Fig. 11 where the ratio $\lambda/\lambda_{\rm FG}$ is plotted. For example, for T13 this quantity stays quite constant with

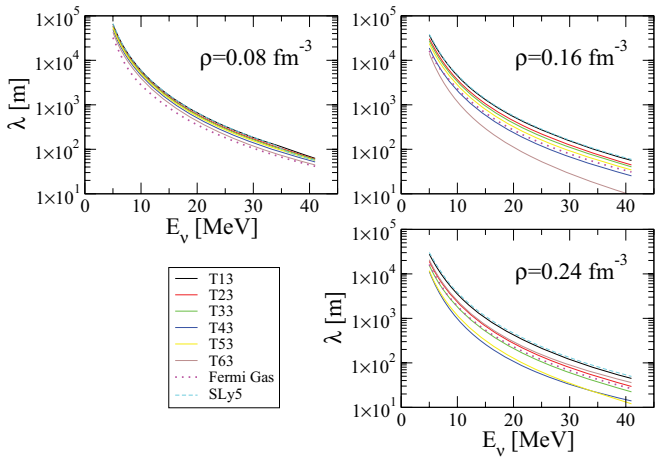

FIG. 10. (Color online) Same as Fig. 9 but for T13–T63 chain.

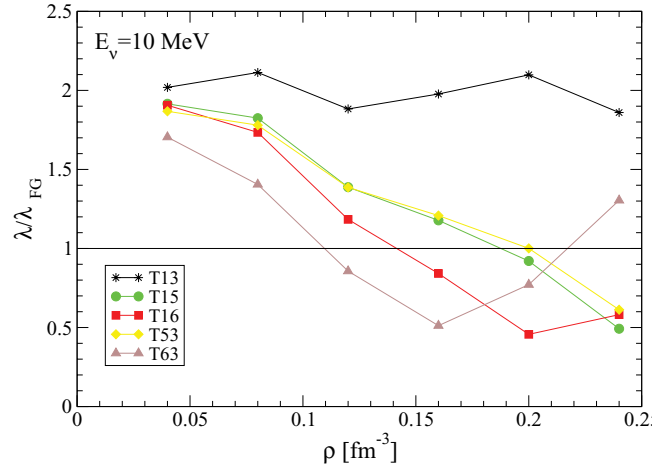

FIG. 11. (Color online) Relative neutrino mean-free path in neutron matter $\lambda/\lambda_{\rm FG}$ as a function of density for some parametrizations of tensor terms. The incoming neutrino energy is $E_\nu = 10$ MeV.

density, for T15 and T53 it decreases, and for T16 and T63 it is no longer monotonic.

IV. SUMMARY AND CONCLUSIONS

In this article we have calculated the RPA response function for pure neutron matter considering Skyrme energy density functionals including tensor terms. This article parallels Refs. [1,2] where similar calculations were performed for the symmetric nuclear matter. As in previous articles, divergences and instabilities of the response [2,45], in particular in the $S = 1$ channel, are discussed in connection with the sum rules.

We applied our results to the study of the neutrino mean-free path. The advantage of the present framework is that it allows us to describe nuclear (and neutron) matter equation of state and the neutrino mean-free path simultaneously, hence in a self-consistent way. Obviously, before achieving a reliable description of neutrino transport phenomena in neutron stars, the calculations performed here must be generalized to finite temperature and for asymmetric nuclear matter. Nonetheless, already at this oversimplified level (pure neutron matter at zero temperature) we have shown the strong dependence of the neutrino mean-free path on the tensor term parametrizations. It represents an important reason, among others, for an accurate treatment of Skyrme functionals including tensor contribution.

ACKNOWLEDGMENTS

This work was supported by the NESQ project (ANR-BLANC 0407). The authors thank M. Ericson and J. Navarro for stimulating and encouraging discussions. The discussions with T. Duguet, M. Bender, and J. Margueron are also acknowledged. We also thank A. Schwenk and F. Braghin for useful comments. M.M. acknowledges the Communauté Française de Belgique (Actions de Recherche Concertées) for financial support.

TABLE I. Contribution of EDF tensor part to residual interaction in terms of B^x coupling constants. For the sake of simplicity we have introduced $\mathbb{K}_{\mathrm{i,j}} = [(k_{12})_i (k_{12})_j]$, where $(k_{12})^{(1)}_M$ is defined in Eq. (9) of article I. The term $\delta_{SS'}\delta_{S1}$ is implicit everywhere.

	$M'=1$	$M'=0$	$M'=-1$
$M=1$	$-2q^2(B^T+4B^{\Delta s})+4B^T\mathbb{K}_{0,0}$ $-4(2B^T+B^F)\mathbb{K}_{1,-1}$	$-4B^F\mathbb{K}_{-1,0}$	$-4B^F\mathbb{K}_{-1,-1}$
$M=0$	$4B^F\mathbb{K}_{0,1}$	$-2q^2(B^T-4B^{\nabla s}+4B^{\Delta s}+B^F)$ $+4(B^T+B^F)\mathbb{K}_{0,0}-8B^T\mathbb{K}_{1,-1}$	$4B^F\mathbb{K}_{-1,0}$
$M=-1$	$-4B^F\mathbb{K}_{1,1}$	$-4B^F\mathbb{K}_{1,0}$	$-2q^2(B^T+4B^{\Delta s})+4B^T\mathbb{K}_{0,0}$ $-4(2B^T+B^F)\mathbb{K}_{1,-1}$

APPENDIX A: PARTICLE-HOLE MATRIX ELEMENTS IN PRESENCE OF A ZERO-RANGE TENSOR INTERACTION

Following the notation adopted in article I and II, we give in Table I the values of the particle-hole residual interaction for the tensor part of the functional in terms of the B^x, with $x = \Delta s, F, \ldots$, coefficients of the functional. This particular notation has been already discussed in article II and we refer to it for detailed explanations.

APPENDIX B: RESPONSE FUNCTIONS

This Appendix contains the explicit expressions for the response functions for pure neutron matter. Since the isospin is no longer a relevant quantum number, each channel is denoted as $(1, M)$ for $S=1$ or only (0) for $S=0$.

We have

(i) for the $S=0$ channel,

$$\frac{\chi_{HF}}{\chi^{(0,0)}_{RPA}} = 1 - \widehat{W}^{(0,0)}_1\chi_0 + W^{(0)}_2\left(\frac{q^2}{2}\chi_0 - 2k_F^2\chi_2\right) + \left[W^{(0)}_2\right]^2 k_F^4\left[\chi_2^2 - \chi_0\chi_4 + \left(\frac{m^*\omega}{k_F^2}\right)^2\chi_0^2 - \frac{m^*}{6\pi^2 k_F}q^2\chi_0\right] + 2\chi_0\left(\frac{m^*\omega}{q}\right)^2\frac{W^{(0)}_2}{1-\frac{m^*k_F^3}{3\pi^2}W^{(0)}_2}, \tag{B1}$$

(ii) for the $S=1$ channels,

$$\frac{\chi_{HF}}{\chi^{(1,0)}_{RPA}} = \left(1+\frac{k_F^3 m^* C^F}{3\pi^2}\right)^2 + \widehat{W}^{(1,0)}_1\chi_0 + W^{(1)}_2\left[\frac{q^2}{2}\left(1+\frac{2C^F k_F^3 m^*}{3\pi^2}\right)\chi_0 - 2k_F^2\chi_2 + \frac{2k_F^5 m^* C^F}{3\pi^2}(\chi_0-\chi_2)\right] + \left[\check{W}^{(1)}_2\right]^2\left[k_F^4\chi_2^2 - k_F^4\chi_0\chi_4 + m^{*2}\omega^2\chi_0^2 - \frac{k_F^3 m^* q^2}{6\pi^2}\chi_0\right] + \frac{2m^{*2}\omega^2}{q^2}\frac{\left(W^{(1)}_2+2C^F\right)\left[1+\frac{k_F^3 m^*}{3\pi^2}X^{(1,0)}\right]}{1+\frac{k_F^3 m^*}{3\pi^2}\left(X^{(1,0)}-W^{(1)}_2-2C^F\right)}\chi_0 \tag{B2}$$

and

$$\frac{\chi_{HF}}{\chi^{(1,\pm1)}_{RPA}} = \left[1-C^F\frac{m^*k_F^3}{6\pi^2}\right]^2 - \widehat{W}^{(1,\pm1)}_1\chi_0 + \left[W^{(1)}_2+C^F\right]\left\{\frac{q^2}{2}\chi_0\left[1-C^F\frac{m^*k_F^3}{3\pi^2}\right] - 2k_F^2\chi_2 - C^F\frac{m^*k_F^5}{3\pi^2}(\chi_0-\chi_2)\right\} + \left[W^{(1)}_2+C^F\right]^2 k_F^4\left\{\chi_2^2-\chi_0\chi_4+\left(\frac{m^*\omega}{k_F^2}\right)^2\chi_0^2 - \frac{m^*}{6\pi^2 k_F}q^2\chi_0\right\} + 2\chi_0\left(\frac{m^*\omega}{q}\right)^2\frac{W^{(1)}_2\left(1+\frac{m^*k_F^3}{3\pi^2}X^{(1,\pm1)}/2\right)}{1-\frac{m^*k_F^3}{3\pi^2}\left[W^{(1)}_2 - X^{(1,\pm1)}/2\right]}. \tag{B3}$$

The coefficients $W^{(\mathrm{S})}_{i=1,2}$ are defined as

$$\begin{aligned}
\tfrac{1}{2}W^{(0)}_1 &= 2\left(C_0^{\rho 0}+C_1^{\rho 0}\right) + (2+\gamma)(1+\gamma)\left(C_0^{\rho\gamma_1}+C_1^{\rho\gamma}\right)\rho^\gamma - \left(2C_0^{\Delta\rho}+2C_1^{\Delta\rho}+\tfrac{1}{2}C_0^\tau+\tfrac{1}{2}C_1^\tau\right)q^2,\\
\tfrac{1}{2}W^{(1)}_1 &= 2\left(C_0^{s,0}+C_0^{s\gamma}\rho_0^\gamma + C_1^{s,0}+C_1^{s\gamma}\rho_0^\gamma\right) - \left(2C_0^{\Delta s}+2C_1^{\Delta s}+\tfrac{1}{2}C_0^T+\tfrac{1}{2}C_1^T\right)q^2,\\
\tfrac{1}{2}W^{(0)}_2 &= C_0^\tau + C_1^\tau, \quad \tfrac{1}{2}W^{(1)}_2 = C_0^T + C_1^T.
\end{aligned} \tag{B4}$$

We have also defined the $\widehat{W}_1^{(\mathrm{S,M})}$ and $X^{(1,\mathrm{M})}$ coefficients as

$$\widehat{W}_1^{(0,0)} = W_1^{(0)} + 4q^4[C^{\nabla J}]^2 \frac{(\beta_2-\beta_3)}{1+q^2(\beta_2-\beta_3)\big[W_2^{(1)}-C^F\big]}, \tag{B5}$$

$$\widehat{W}_1^{(1,0)} = -\big[W_1^{(1)} + 4q^2 C^{\nabla s}\big] + C^F\left[q^2 - 4\left(\frac{m^*\omega}{q}\right)^2\right] + m^*\rho[C^F]^2\left[2k_F^2 + \frac{1}{2}q^2 - \frac{2}{k_F^2}\left(\frac{m^*\omega}{q}\right)^2\right], \tag{B6}$$

$$\begin{aligned}\widehat{W}_1^{(1,\pm1)} &= W_1^{(1)} + 2q^4[C^{\nabla J}]^2 \frac{(\beta_2-\beta_3)}{1+q^2(\beta_2-\beta_3)\big[W_2^{(0)}\big]} - 2C^F\left(\frac{m^*\omega}{q}\right)^2 \\ &\quad + [C^F]^2\left(\frac{1}{2}q^2 m^*\rho + \frac{1}{16}\left[q^2 - 4\left(\frac{m^*\omega}{q}\right)^2\right]^2\chi_0 - \frac{1}{2}k_F^2\left[q^2 + 4\left(\frac{m^*\omega}{q}\right)^2\right]\chi_2 + k_F^4\chi_4\right),\end{aligned} \tag{B7}$$

$$X^{(1,0)} = 2q^2[C^F]^2 \frac{(\beta_2-\beta_3)}{1+q^2(\beta_2-\beta_3)\big[W_2^{(1)}+3C^F\big]}, \tag{B8}$$

$$X^{(1,\pm1)} = 2q^2[C^F]^2 \frac{(\beta_2-\beta_3)}{1+q^2(\beta_2-\beta_3)W_2^{(1)}}. \tag{B9}$$

APPENDIX C: LANDAU APPROXIMATION

Since we have no isospin quantum number, the p-h interaction is reduced to three terms. As done in article II we take the limit $q \to 0$ and $\mathbf{q}_{1,2} \to \mathbf{k}_F$ of the second functional derivative and we obtain

$$\begin{aligned}V_{\mathrm{ph}}^{\mathrm{Landau}}(\mathbf{k}_F,\mathbf{k}_F) &= \frac{1}{2}W_{1,L}^{(0)} + \frac{1}{2}W_{1,L}^{(1)}\boldsymbol{\sigma}_a\cdot\boldsymbol{\sigma}_b \\ &\quad + \frac{1}{2}\big[W_{2,L}^{(0)} + W_{2,L}^{(1)}\boldsymbol{\sigma}_a\cdot\boldsymbol{\sigma}_b\big]2k_F^2\,[1-\cos\theta] \\ &\quad + \frac{2}{3}k_F^2 C^F\,[1-\cos\theta]\,\boldsymbol{\sigma}_a\cdot\boldsymbol{\sigma}_b \\ &\quad + \frac{k_F^2}{3}C^F\frac{k_{12}^2}{k_F^2}S_{ab},\end{aligned} \tag{C1}$$

where the symbols S_{ab} has been defined in Refs. [46,47]. The various $W_{i,L}^{(S)}$ coefficients with $i = 1, 2$ can be easily calculated from the $W_i^{(S)}$ coefficients defined in Eq. (B4) taking the limit of $W_i^{(S)}$ for $q \to 0$.

So the Landau parameters can be written as

$$\begin{aligned}N_0^{-1}F_0 &= \tfrac{1}{2}W_{1,L}^{(0)} + k_F^2 W_{2,L}^{(0)}, \\ N_0^{-1}F_1 &= -k_F^2 W_{2,L}^{(0)}, \\ N_0^{-1}G_0 &= \tfrac{1}{2}W_{1,L}^{(1)} + k_F^2 W_{2,L}^{(1)} + \tfrac{2}{3}k_F^2 C^F, \\ N_0^{-1}G_1 &= -k_F^2 W_{2,L}^{(1)} + \tfrac{2}{3}k_F^2 C^F, \\ N_0^{-1}H_0 &= \tfrac{1}{3}k_F^2 C^F,\end{aligned}$$

where $N_0^{-1} = 2\pi^2/(gm^*k_F)$ is the normalization factor and $g = 2$ is the degeneracy in PNM.

[1] D. Davesne, M. Martini, K. Bennaceur, and J. Meyer, Phys. Rev. C **80**, 024314 (2009); **84**, 059904(E) (2011).
[2] A. Pastore, D. Davesne, Y. Lallouet, M. Martini, K. Bennaceur, and J. Meyer, Phys. Rev. C **85**, 054317 (2012).
[3] M. Kortelainen, T. Lesinski, J. Moré, W. Nazarewicz, J. Sarich, N. Schunck, M. V. Stoitsov, and S. Wild, Phys. Rev. C **82**, 024313 (2010).
[4] M. Kortelainen, J. McDonnell, W. Nazarewicz, P.-G. Reinhard, J. Sarich, N. Schunck, M. V. Stoitsov, and S. M. Wild, Phys. Rev. C **85**, 024304 (2012).
[5] S. Marcos, R. Niembro, M. L. Quelle, and J. Navarro, Phys. Lett. B **271**, 277 (1991).
[6] S. Fantoni, A. Sarsa, and K. E. Schmidt, Phys. Rev. Lett. **87**, 181101 (2001).
[7] J. Margueron, J. Navarro, and Nguyen Van Giai, Phys. Rev. C **66**, 014303 (2002).
[8] I. Vidana, A. Polls, and A. Ramos, Phys. Rev. C **65**, 035804 (2002).
[9] I. Vidana and I. Bombaci, Phys. Rev. C **66**, 045801 (2002).
[10] A. A. Isayev and J. Yang, Phys. Rev. C **69**, 025801 (2004).
[11] A. Beraudo, A. De Pace, M. Martini, and A. Molinari, Ann. Phys. (NY) **311**, 81 (2004).
[12] A. Beraudo, A. De Pace, M. Martini, and A. Molinari, Ann. Phys. (NY) **317**, 444 (2005).
[13] A. Rios, A. Polls, and I. Vidana, Phys. Rev. C **71**, 055802 (2005).
[14] I. Bombaci, A. Polls, A. Ramos, A. Rios, and I. Vidana, Phys. Lett. B **632**, 638 (2006).
[15] D. Lopez-Val, A. Rios, A. Polls, and I. Vidana, Phys. Rev. C **74**, 068801 (2006).
[16] F. Sammarruca and P. G. Krastev, Phys. Rev. C **75**, 034315 (2007).
[17] G. H. Bordbar and M. Bigdeli, Phys. Rev. C **77**, 015805 (2008).
[18] J. Margueron and H. Sagawa, J. Phys. G **36**, 125102 (2009).
[19] A. A. Isayev and J. Yang, Phys. Rev. C **80**, 065801 (2009).
[20] N. Chamel and S. Goriely, Phys. Rev. C **82**, 045804 (2010).
[21] F. L. Braghin, D. Vautherin, and A. Abada, Phys. Rev. C **52**, 2504 (1995).

[22] N. Iwamoto and C. J. Pethick, Phys. Rev. D **25**, 313 (1982).
[23] S. Reddy, M. Prakash, J. M. Lattimer, and J. A. Pons, Phys. Rev. C **59**, 2888 (1999).
[24] J. Navarro, E. S. Hernandez, and D. Vautherin, Phys. Rev. C **60**, 045801 (1999).
[25] C. Shen, U. Lombardo, Nguyen Van Giai, and W. Zuo, Phys. Rev. C **68**, 055802 (2003).
[26] J. Margueron, I. Vidaña, and I. Bombaci, Phys. Rev. C **68**, 055806 (2003).
[27] J. Margueron, Nguyen Van Giai, and J. Navarro, Phys. Rev. C **74**, 015805 (2006).
[28] G. I. Lykasov, C. J. Pethick, and A. Schwenk, Phys. Rev. C **78**, 045803 (2008).
[29] S. Bacca, K. Hally, C. J. Pethick, and A. Schwenk, Phys. Rev. C **80**, 032802 (2009).
[30] T. Lesinski, M. Bender, K. Bennaceur, T. Duguet, and J. Meyer, Phys. Rev. C **76**, 014312 (2007).
[31] J. Dobaczewski, H. Flocard, and J. Treiner, Nucl. Phys. A **422**, 103 (1984).
[32] J. Bartel, P. Quentin, M. Brack, C. Guet, and H. B. Hakansson, Nucl. Phys. A **386**, 79 (1982).
[33] Nguyen Van Giai and H. Sagawa, Phys. Lett. B **106**, 379 (1981).
[34] E. Chabanat, P. Bonche, P. Haensel, J. Meyer, and R. Schaeffer, Nucl. Phys. A **627**, 710 (1997).
[35] E. Chabanat, P. Bonche, P. Haensel, J. Meyer, and R. Schaeffer, Nucl. Phys. A **635**, 231 (1998).
[36] E. Chabanat, P. Bonche, P. Haensel, J. Meyer, and R. Schaeffer, Nucl. Phys. A **643**, 441(E) (1998).
[37] M. Samyn, S. Goriely, and J. M. Pearson, Phys. Rev. C **72**, 044316 (2005).
[38] P.-G. Reinhard, D. J. Dean, W. Nazarewicz, J. Dobaczewski, J. A. Maruhn, and M. R. Strayer, Phys. Rev. C **60**, 014316 (1999).
[39] O. Bohigas, A. M. Lane, and J. Martorell, Phys. Rep. **51**, 267 (1979).
[40] E. Lipparini and S. Stringari, Phys. Rep. **175**, 103 (1989).
[41] M. Martini, M. Ericson, G. Chanfray, and J. Marteau, Phys. Rev. C **80**, 065501 (2009).
[42] C. J. Horowitz, Phys. Rev. D **65**, 043001 (2002).
[43] Y. Chen, Y. Yuan, and Y. Liu, Phys. Rev. C **79**, 055802 (2009).
[44] M. Martini, M. Ericson, G. Chanfray, and J. Marteau, Phys. Rev. C **81**, 045502 (2010).
[45] A. Pastore, K. Bennaceur, D. Davesne, and J. Meyer, Int. J. Mod. Phys. E **21**, 1250040 (2012).
[46] K. F. Liu, Nuovo Cimento A **70**, 329 (1982).
[47] L.-G. Cao, G. Colò, and H. Sagawa, Phys. Rev. C **81**, 044302 (2010).